Configuration dependent critical nuclei in the self assembly of magic clusters

W. J. Ong[ab] and E. S. Tok*[ab]

Received 15th November 2006, Accepted 7th December 2006
First published as an Advance Article on the web 2nd January 2007
DOI: 10.1039/b616739j

Evidence for the formation of various 2-D structures possessing different numbers of Co–Si magic clusters (size $\sim 10.0 \pm 0.5$ Å), configurations and lifetimes are studied in real time on a Si(111)-(7 × 7) surface at elevated temperature in the STM. Observations of individual cluster diffusion, attachment and detachment dynamics resolve unequivocally the question of self assembly over surface reconstruction. The smallest stable structure consisting of seven individual Co–Si magic clusters arranged in a hexagonal closed packed formation ($i = 7$) is found to retain sufficient cohesive energy to avoid dissociation. A configuration dependent critical 2-D nuclei ($i^* = 6$) is determined to exist in facilitating the self assembly dynamics.

Self assembly is an alternative and promising route to creating mono-dispersed nano-sized structures on surfaces of materials.[1–5] These unique structures are often found to comprise a collection of a specific number of adatoms (magic clusters) and they exist not only in diverse homogeneous metallic (*e.g.* Ag/Ag(100) and Pt/Pt(110))[6,7] and semiconducting (*e.g.* Si/Si(111)) systems[8–10] but also in heterogeneous systems consisting of mixed metal/semi-conducting materials (*e.g.* In/Si(001) and Ga, In, Ag, Mn or Pb/Si(111)).[11–14] To harness these structures as potential building blocks for nanoscopic devices or as templates for nano-fabrication in terms of control over size, distribution and ordering, requires a fundamental understanding of the magic cluster self assembly dynamics. Hence it is of interest to co-relate this phenomenon with respect to individual cluster dynamics and its evolution in relation to the cluster–cluster interactions and configurations. In fact reported works so far in general have assumed that the ordering of clusters occurs spontaneously and have not addressed whether a stable critical nuclei exists to promote the self assembly process, analogous to that in thin film growth.[15–18] Evidence for the existence of such a critical nuclei would also resolve the question of whether these periodic arrangements are due to self assembly of individual clusters on the surface or an intrinsic surface reconstruction.

In this study, we will attempt to address these issues for a metal/semiconductor material system by providing dynamic STM evidence of "Co–Si" magic cluster diffusion and attachment/detachment behavior during the formation of different 2-D cluster arrangements with varying lifetimes on a Si(111)-(7 × 7) surface at elevated temperatures. In particular, we introduce the idea of a configuration dependent critical 2-D nucleus which is directly responsible for the self alignment of magic clusters. An Omicron VT-STM is used to study the Si(111) sample which was cleaned by *in situ* flashing to 1200 °C to obtain well ordered (7 × 7) reconstructed surface. Co was deposited onto the surface at room temperature *via* a solid source Electron Beam Evaporator. The various surface structures were obtained by direct current heating to the respective temperatures measured with an optical pyrometer. The STM bias used ranges typically from ±0.1 to 3.0 V with tunneling currents of ~0.1 nA.

We first deposited 1 ML of Co at room temperature onto a clean (7 × 7)-Si(111) surface as shown in Fig. 1a. Heating this surface to 460 °C yields the formation of identically sized and shaped spherical features (size $\sim 10.0 \pm 0.5$ nm) which we label as "Co–Si" magic clusters (Fig. 1b). While these clusters dominate the surface morphology in a random manner, it is interesting to note that some of the clusters gather into close packed hexagonal formations, as indicated in Fig. 1b inset. Further annealing of the surface to 610 °C appears to extend the cluster ordering (Fig. 1c and inset) leading to the formation of 2-D "Co–Si" magic cluster arrays with a $\sqrt{7} \times \sqrt{7}$ unit cell as indicated by our line profile analysis of cluster separation which was found to be $\sqrt{7}$ times that of (1 × 1)-Si(111). This evolution suggests that the clusters could be mobile. Therefore in order to investigate this more closely, we deposited a lower coverage (0.5 ML) of Co onto another clean Si(111)-(7 × 7).

Fig. 1d shows the same occurrence of "Co–Si" magic clusters after annealing to 460 °C for 30 min. The clusters are seen to be randomly distributed over the (7 × 7)-Si(111) reconstructed surface albeit at a lower cluster density count compared with Fig. 1b. At this lower coverage, the STM scans not only show individual and paired clusters but also gathering of clusters to form various geometries consisting of different number of clusters, *i*. At 460 °C, individual ($i = 1$) clusters appear to dominate the surface in spite of the existence of paired ($i = 2$) clusters, cluster trimers ($i = 3$) and triangular configurations ($i = 4$) (highlighted in Fig. 1e as A, B and C). By annealing this surface to 490 °C, ring formations ($i = 6$), hexagonal structures ($i = 7$) and domains of clusters where $i > 7$ (these features are highlighted in Fig. 1e as D, E and F, respectively) can now be clearly observed. When the surface

[a] *Department of Physics, National University of Singapore, Singapore, 119260, Singapore. E-mail: phytokes@nus.edu.sg; Tel: ++65-6874-1192. E-mail: wj-ong@imre.a-star.edu.sg*
[b] *Institute of Materials Research and Engineering, IMRE Building, 3 Research Link, Singapore, 117602, Singapore*

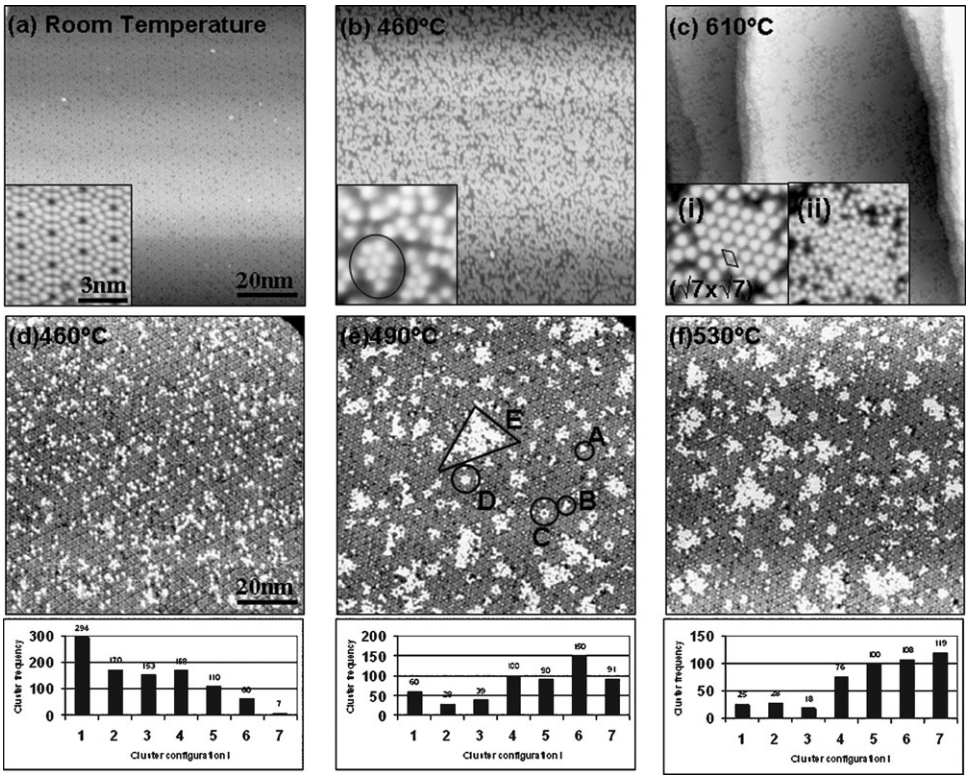

Fig. 1 (a)–(c) show 100 × 100 nm STM scans with 8 × 8 nm inset images of (a) clean (7 × 7)-Si(111) surface, (b) 1 ML of Co deposited at room temperature (RT) and annealed to 460 °, and (c) surface with ($\sqrt{7} \times \sqrt{7}$) unit cell after annealing to 610 °C (inset shows dual bias scans at (i) −2.4 V and (ii) +2.4 V). Fig. 1d–f shows same size STM scans with histograms tracing the occurrences of $i = 1$ to 7, after 0.5 ML of Co is deposited at RT and annealed for the 30 min to (d) 460 °C, (e) 490 °C and (f) 530 °C. The configurations $i = 3$, 4, 6, 7 and domains of clusters where $i > 7$ are highlighted as A, B, C, D and E, respectively, in Fig. 1e.

is further annealed to 530 °C (Fig. 1f), we observe occurrences of even less single or paired clusters while more clusters now exist as ring ($i = 6$), hexagonal ($i = 7$) or cluster domain ($i > 7$) configurations. This evolution of cluster configuration as a function of annealing temperature is also represented in the corresponding histograms as shown in Fig. 1d–f, which clearly indicates a preferential occurrence of $i = 6$ and 7 over $i = 1$ to 5 at higher temperatures. We note that cluster density is conserved throughout the various annealing temperatures, which suggests that the clusters are mobile and exhibit an energetic preference to gather into localized 2-D ordered arrangements.

As the present data are room temperature snap shots of the self assembly process frozen at various stages of annealing, a *real time* study is necessary to probe the significance of these various 2-D configurations, in particular, the cluster dynamics leading to the evolution of $i = 6$ and 7 on the (7 × 7) surface. We first prepare a surface similar to Fig. 1b and operate the VT-STM in a fast scanning mode, where each scan size of 8 by 8 nm was recorded in quick 5 s time frames, to capture the self assembly process in real time at 400 °C. As each frame consists of 500 horizontal scan lines taken over 5 s, the resolution of this scanning speed would take approximately 0.01 s to complete 1 line scan.

The data capturing the cluster dynamics in forming ring structures of $i = 6$ and hexagonal structures of $i = 7$ clusters are shown in Fig. 2a–i and 3a–h, respectively. Fig. 2a–c shows the assembly of 5 clusters (including a cluster labeled "X") self adjusting to achieve equal cluster–cluster separation leaving one vacancy along the boundary of a (7 × 7) half unit cell. A sixth cluster identified as "Y" is also seen in the vicinity (Fig. 2c), which is later observed in Fig. 2-D to occupy this vacancy to complete a ring-like structure consisting of $i = 6$ clusters. This configuration appears to be stable within the next scan duration (Fig. 2e). However, a cluster is observed to detach and move away from the ring structure in the following frame (Fig. 2f). A shift in the position of cluster "X" collapses the original ring structure (Fig. 2g) leading to the departure of two more clusters as observed in Fig. 2h–i. The assembly of clusters to form this $i = 6$ configuration in this instance is not stable within the time frame of the STM scans.

Fig. 3a–b shows the self assembly of 6 clusters to form the ring-like structure ($i = 6$) similar to Fig. 2d and e. Unlike the previous observation (Fig. 2f), one of the clusters, as shown in Fig. 3c, moves to occupy the vacant site in the centre of the ring structure. In the next frame (Fig. 3d), a seventh cluster is observed to have attached itself to the ring structure and moves preferentially to occupy the vacancy to complete a compact hexagonal structure comprising $i = 7$ as shown in Fig. 3e. Unlike the previous STM scans (Fig. 2), this particular configuration appears to be a more stable arrangement as it persists without dissociation in subsequent STM frames (Fig. 3e–h). It appears to retain sufficient lifetime for individual diffusing clusters to be observed within the vicinity.

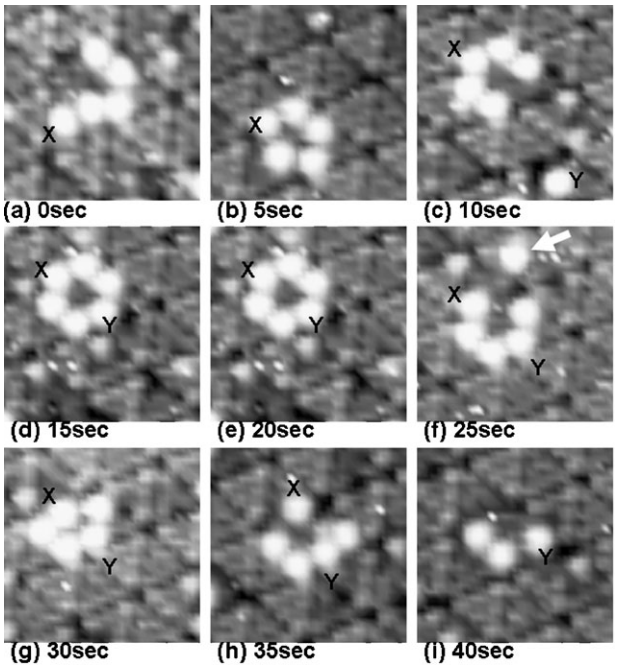

Fig. 2 (a)–(i) show high speed 8 × 8 nm STM scans captured in 5 s frames of the formation and dissociation of a $i = 6$ configuration at 400 °C on a surface.

We were also able to capture the cluster dynamics of an $i = 4$ cluster configuration in proximity to an $i = 7$ structure. Fig. 4a–d shows the assembly of clusters first forming an $i = 3$ trimer configuration which subsequently evolves to an $i = 4$ triangular shaped cluster configuration (the centre cluster position is marked by an arrow). However as shown in Fig. 4f–g, this $i = 4$ grouping is not stable as it is observed to dissociate and diffuse away its original site (marked by the arrow), while the $i = 7$ structure remains intact. The observation of cluster attachment and detachment is thus unlikely to be tip induced.

From the STM scans shown in Fig. 2 to 4, the $i = 7$ arrangement of clusters is clearly a more stable configuration and this is also demonstrated by its dominant occurrence at higher temperatures as shown by the histograms in Fig. 1d–f. This is not unexpected as the clusters within the $i = 7$ configuration are arranged in a hexagonal closed packed formation, which maximizes cluster co-ordination and minimizes surface dangling bonds on an underlying Si(111)-(7 × 7) template. The key step leading to the formation of $i = 7$ is captured in Fig. 3c, where one of the clusters from the original $i = 6$ ring structure diffuses inward to occupy the centre vacancy instead of dissociating in Fig. 2f, as indicated by the arrows shown in the respective figures. This occupation of the centre site within the $i = 6$ configuration would also lead to higher co-ordination between clusters due to a greater complement of neighboring clusters (closed packing) which is more stable than the open ring arrangement (Fig. 2e or 3b). In this arrangement, it could most easily accommodate additional clusters to eventually form the stable $i = 7$ configuration (Fig. 3c–e) for hexagonal closed packing to occur. Hence the formation of a more closed-packed $i^* = 6$ configuration is identified as an essential step (as shown in Fig. 3c), existing as a critical nuclei preceding the formation of the smallest stable configuration of clusters ($i = 7$). The average cluster separation of this $i = 7$ configuration is found to be $\sim 10.0 \pm 1.0$ Å which is $\sim\sqrt{7}$ times the periodicity of Si(111)-(1 × 1). The attachment of additional clusters will thus to lead to the propagation of $(\sqrt{7} \times \sqrt{7})$ cluster domain ordering as observed in Fig. 1.

The direct observation of cluster dynamics shown in Fig. 2, 3 and 4, also allows us to estimate the lifetime for each respective configuration ($i = 4$, 5, 6 and 7) prior to cluster detachment. In comparison, the $i = 7$ configuration (Fig. 3e–h) clearly has a lifetime that is longer than 20 s, which is much greater than the lifetime for $i = 6$ (Fig. 2d–f), $i = 5$ (Fig. 2g–i) and $i = 4$ (Fig. 4d–f). Although the present high speed STM scans are unable to resolve the individual lifetimes for $i = 6$, 5 and 4, these configurations clearly do not exist beyond 5 to 10 s. Using the Frenkel equation for lifetime ($\tau = \tau_o \exp[E_b/kT]$, assuming $\tau_o = 10^{-13}$ s), the binding energy (E_b) of these configurations of clusters are estimated to be approximately between 1.83 and 1.85 eV.

At the same time, the observation of individual cluster diffusion on the terrace would also enable us to estimate the diffusion barrier by measuring the mean square displacement $\langle x^2 \rangle$ of clusters. At 400 °C, $\langle x^2 \rangle$ was determined to be

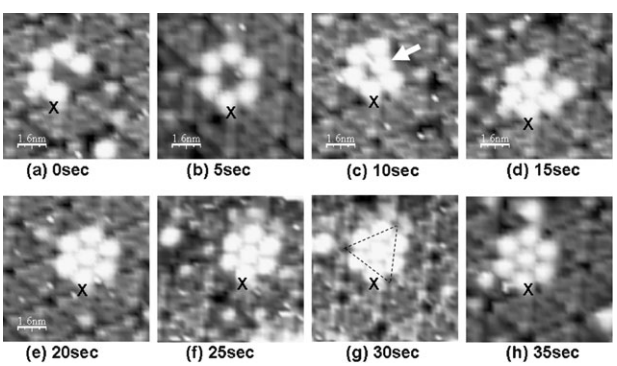

Fig. 3 (a)–(h) show high speed 8 × 8 nm STM scans of the formation of a stable $i = 7$ configuration *via* a critical nuclei $i^* = 6$ (with cluster "X" as a point of reference) as shown in Fig. 3c at 400 °C captured in 5 s frames.

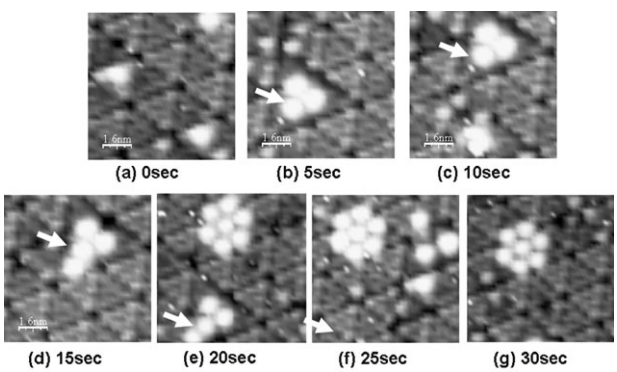

Fig. 4 (a)–(g) show high speed 8 × 8 nm STM scans of the formation of $i = 4$ co-existing with $i = 7$ configuration at 400 °C captured in 5 s frames. The centre cluster position is marked by an arrow as a fixed point of reference.

$\sim 11.7 \times 10^{-18}$ m^2. Since the mean square displacement and Arrhenius expressions for diffusion co-efficient (D) are related as follows;

$$\langle x^2 \rangle \sim Dt \quad (1)$$

$$D = D_o \exp[-E_d/k_b T] \quad (2)$$

$$D_o = \gamma_o a_o^2 \quad (3)$$

where E_d is the diffusion barrier, t is time taken (5 s), T is the substrate temperature, k_b is the Boltzman constant, γ_o is the pre-factor (10^{13} s^{-1}) and a_o is the lattice parameter (3.8 Å), E_d was thus estimated to be ~ 1.6 eV.

The binding energy of these cluster configurations, $i = 4$, 5 and 6 ($E_b \sim 1.83$ to 1.85 eV), is thus comparable to the diffusion barrier of a single cluster ($E_d \sim 1.6$ eV) over the Si(111)-(7 × 7) surface. Hence these configurations are likely to be more susceptible to cluster detachment than $i = 7$ and even more so at progressively higher temperatures. This is consistent with the histogram data (Fig. 1d–f) which show predominant occurrence of $i \geq 7$ compared to the other configurations (*i.e.* $i < 7$) at higher temperatures.

Our data thus far show that the critical nuclei $i^* = 6$ must first form, before the stable $i = 7$ configuration can exist to propagate cluster ordering *via* further individual cluster diffusion and attachment. Hence the cluster ordering with a unit cell of ($\sqrt{7} \times \sqrt{7}$) observed in Fig. 1c does not occur spontaneously. Individual clusters are observed to diffuse as a whole cluster entity and it appears to glide on the (7 × 7) surface. This behavior is dissimilar to earlier diffusion mechanism such as sequential displacement of adatoms at cluster edges (*e.g.* Rh/Rh(100)[19]), "leap-frog" diffusion modes (*e.g.* Pt adatom at the end of cluster displaces across the cluster to the front on a Pt(110) surface[20]) and dimer shear motion of compact clusters on metal (100) surfaces.[21] In order to deduce a plausible diffusion mechanism to describe the observed motion of the cluster, structural elucidation of the "Co–Si" magic cluster would be required. Using STM dual biasing data (Fig. 1c inset), the clusters which appear as bright protrusions (negative bias) can be resolved into a ring-like appearance consisting of 3 smaller round protrusions with a dark centre depression (positive bias). This finding is similar to that reported in ref. 22 and 23, in which structural models have been proposed. The "Co–Si" cluster in ref. 22 is described as a 7-atom cluster comprising one Co atom encapsulated within 6 Si atoms (3 Si atoms bridging and 3 Si atoms capping) arranged as a ($\sqrt{7} \times \sqrt{7}$) reconstruction on a (1 × 1) template. As for the cluster structure reported in ref. 23, it is described as a 9-atom cluster comprising 3 Si atoms on top of 6 Co atoms which are bonded down to the Si rest atoms below, within a (7 × 7) half unit cell instead. The difference between the two models is that one sits on a (1 × 1) template[22] while the latter is built upon on a (7 × 7) template[23] and is consequently more akin to our present work. This structure has not only been shown to be energetically stable through first principles total energy calculations but also fits the STM/STS experimental measurements.[23] In order for this cluster to diffuse, we propose that the process would need to involve (i) exchange of Si atoms between the top layer of the cluster and the underlying adatom layer of the (7 × 7)-DAS structure and (ii) the sequential breaking and formation of bonds between the base Co atoms of the cluster with the (7 × 7)-DAS Si rest atoms.

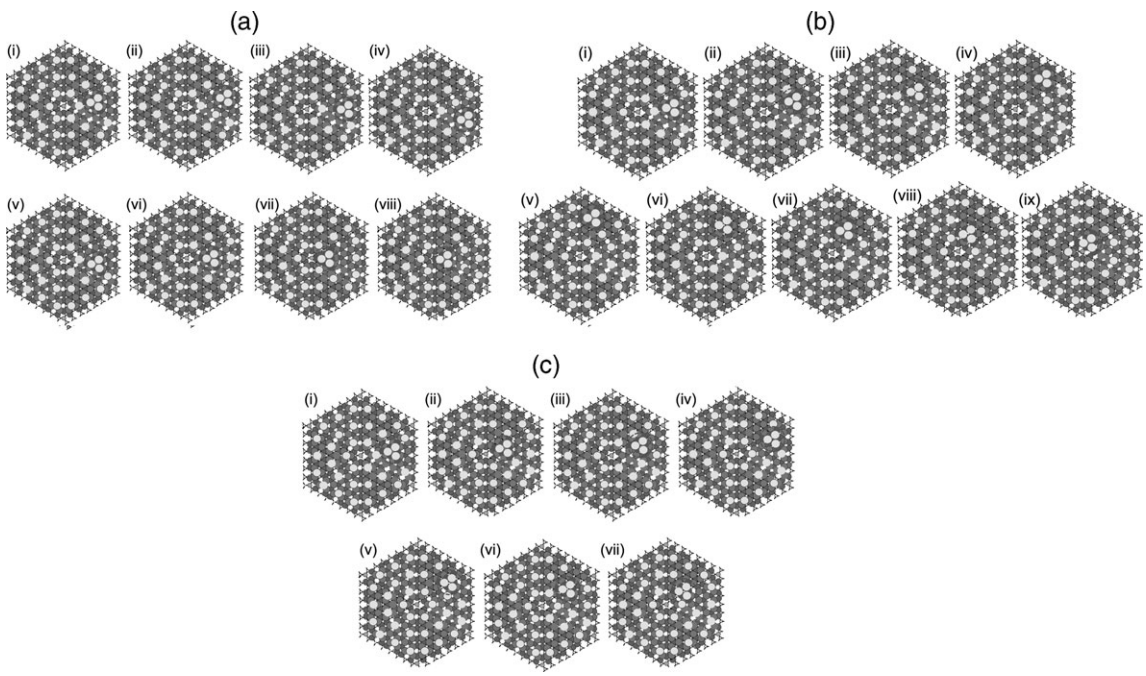

Fig. 5 Schematic diagrams for the plausible exchange diffusion process of a Co–Si cluster structure while preserving the underlying (7 × 7) template. Fig. 5a(i)-(viii) shows cluster moving within faulted half of (7 × 7) unit cell. Fig. 5b(i)–(ix) shows cluster crossing into and moving within the unfaulted half of the (7 × 7) unit cell. Fig. 5c(i)-(vii) shows cluster moving along and crossing the boundary separating the faulted and unfaulted halves of the (7 × 7) unit cell.

We illustrate this process schematically in Fig. 5a–c for a cluster moving within the faulted half, unfaulted half and across the (7 × 7) unit cell boundary, respectively. While we were not able to resolve this diffusion-exchange mechanism in the present work, the resultant diffusion mechanism proposed would allow the cluster structure to diffuse not only as a single entity in a gliding motion but also to occur without disrupting the underlying (7 × 7) template, as seen in our STM data.

In conclusion, we have addressed the dynamical behavior of these magic clusters (size $\sim 10.0 \pm 0.5$ Å) leading to the self organization and ordering on a Si(111)-(7 × 7) template. Evidence of individual cluster diffusion, formation of various 2-D structures possessing different numbers of Co–Si magic clusters (i = 4, 5, 6 and 7), configurations and lifetimes resolve the self assembly process. It does not occur spontaneously and a configuration dependent critical nuclei (i^* = 6) exists, parallel to the role of a critical nuclei in the nucleation theory of thin film growth.[18–21] The smallest stable configuration is one consisting of seven Co–Si magic clusters arranged in a hexagonal closed packed formation (i = 7). This hexagonal closed packed formation not only maximizes cluster co-ordination but also minimizes surface dangling bonds on an underlying Si(111)-(7 × 7) template. Finally, in contrast with traditional growth concepts, the "growth" of these cluster structures is translated *via* diffusion, attachment and self alignment of a magic clusters instead of adatoms.

Acknowledgements

We thank Prof. ACH Huan for support and gratefully acknowledge the financial support from NUS and IMRE under the Atomic Layer Epitaxy Programme.

References

1 H. Roder, E. Hahn, H. Brune, J. P. Bucher and K. Kern, *Nature*, 1993, **366**, 141.
2 J. A. Jenson, C. Yan and A. C. Kummel, *Science*, 1995, **267**, 493.
3 S. Chiang, *Science*, 1996, **272**, 1123.
4 H. Brune, M. Giovannini, K. Broman and K. Kern, *Nature*, 1998, **394**, 451.
5 T. Ito and S. Okazaki, *Nature*, 2000, **406**, 1027.
6 J. M. Wen, S. L. Chang, J. W. Burnett, J. W. Evans and P. A. Thel, *Phys. Rev. Lett*., 1994, **73**, 2591.
7 T. R. Linderoth, S. Horch, L. Peterson, S. Helveg, E. Laegsgaard, I. Stensgaard and F. Besenbacher, *Phys. Rev. Lett*., 1999, **82**, 1494.
8 G. Rosenfield, A. F. Becker, B. Poelsema, L. K. Verheij and G. Cosma, *Phys. Rev. Lett*., 1992, **69**, 917.
9 S. K. Nayak, P. Jena, V. S. Stepanyuk, W. Hergert and K. Wildberger, *Phys. Rev. B*, 1997, **56**, 6952.
10 I.-S. Hwang, M.-S. Ho and T. T. Tsong, *Phys. Rev. Lett*., 1999, **83**, 120.
11 M. Y. Lai and Y. L. Wang, *Phys. Rev. Lett*., 1998, **81**, 164.
12 J. L. Li, J. F. Jia, X. J. Liang, X. Liu, J. Z. Wang, Q. K. Xue, Z. Q. Li, J. S. Tse, Z. Zhang and S. B. Zhang, *Phys. Rev. Lett*., 2002, **88**, 066101–1.
13 V. G. Kotlyar, A. V. Zotov, A. A. Saranin, E. N. Chukurov, T. V. Kasyanov, M. A. Cherevik, I. V. Pisarenko, H. Okado, M. Katayama, K. Oura and V. G. Lifshits, *Phys. Rev. Lett*., 2003, **91**, 26104–1.
14 S. C. Li, J. F. Jia, R. F. Dou, Q. K. Xue, I. G. Batyrev and S. B. Zhang, *Phys. Rev. Lett*., 2004, **93**, 116103–1.
15 J. A. Venebles, G. D. T. Spiller and M. Hanbucken, *Rep. Prog. Phys*., 1984, **47**, 399.
16 Z. Y. Zhang and M. G. Lagally, *Science*, 1997, **276**, 377.
17 H. Brune, *Surf. Sci. Rep*., 1998, **31**, 121.
18 J. V. Barth, G. Costantini and K. Kern, *Nature*, 2005, **437**, 671.
19 G. L. Kellog, *Prog. Surf. Sci*., 1996, **53**, 217.
20 T. R. Linderoth, S. Horch, L. Peterson, E. Laegsgaard, I. Stensgaard and F. Besenbacher, *New J. Phys*., 2005, **7**, 13.
21 Z. P. Shi, Z. Zhang, A. K. Swan and J. F. Wendelken, *Phys. Rev. Lett*., 1996, **76**, 4927.
22 M. H. Tsai, J. D. Dow, P. A. Bennett and D. G. Cahill, *Phys. Rev. B*, 1993, **48**, 2486.
23 M. A. K. Zilani, Y. Y. Sun, H. Xu, Lei Liu, Y. P. Feng, X.-S. Wang and A. T. S. Wee, *Phys. Rev. B*, 2005, **72**, 193402.